A study of the Raman spectrum of CO_2 using an algebraic approach

M. Sánchez-Castellanos[1], R. Lemus[1], M. Carvajal[2†], F. Pérez-Bernal[2†], J.M. Fernández[3]

[1] Instituto de Ciencias Nucleares, Universidad Nacional Autónoma de México, Apartado Postal 70-543, 04510 México, DF, Mexico.

[2] Departamento de Física Aplicada, Unidad Asociada al CSIC, Facultad de Ciencias Experimentales, Universidad de Huelva, Avenida de las Fuerzas Armadas, s/n 21071, Huelva, Spain.

[3] Instituto de Estructura de la Materia, IEM-CSIC, Serrano 121, Madrid 28006, Spain.

Keywords: Raman spectrum, carbon dioxide, CO_2, molecular polarizability, algebraic approach.

Abstract

The vibrational Raman spectrum of CO_2 is calculated by means of the algebraic model $U(2) \times U(3) \times U(2)$. The Hamiltonian and the molecular polarizability tensor operators are expanded in terms of symmetry coordinates, which in turn are transformed into the algebraic representation. The derivatives of the polarizability with respect to symmetry coordinates are fitted to six experimental transition intensities at room temperature and compared with previous experimental and *ab initio* values. The Raman spectrum of the Fermi diad at 1750 K is then simulated and compared with the experimental one.

1. Introduction

An algebraic description of the vibrational excitations of carbon dioxide (CO_2) in its ground electronic state has been recently reported [1, 2]. The novel contribution of that work is the use of a polyad-preserving local-mode model to describe a molecule with a strong normal-mode behavior, taking advantage of the inclusion of anharmonic effects from the outset [3]. In Refs. [1, 2] a set of 101 experimental vibrational energies were fitted with a root mean square deviation of 0.53 cm^{-1}. This description can be considered accurate for the standards of vibrational spectroscopy. However, the eigenstates provided by the model should be tested, since a good energy fit alone does not guarantee the wave functions quality [4]. E.g., for the carbon dioxide, a change of sign of the Fermi interaction coefficient yields vibrational energy levels of the same quality although with quite different wavefunctions.

The analysis of transition probabilities is the natural arena to test the wavefunctions. Regarding vibrational excitations, infrared and Raman spectroscopy provide the experimental data needed to achieve this goal. In a recent work, the Raman spectrum of CO_2 at 1750 K from a methane/air flame in the $1150 - 1460$ cm^{-1} range was reported [5]. This spectrum can be used to test the vibrational wavefunctions as long as a suited description of the dependence of the molecular polarizability tensor on the vibrational motions is available. Tejeda *et al.* expanded the mean polarizability into a Taylor series of the normal coordinates [6] and determined its main derivatives by fitting a set of selected experimental transition moments.

In this work we simulate theoretically the Raman spectrum obtained experimentally in Ref. [5]. To this end we use the eigenstates provided by the $U(2) \times U(3) \times U(2)$ model to compute the transition moments of the mean polarizability. A selected set of six transitions having the largest transition moments are used to fit, according to our model, the derivatives of the mean polarizability with respect to the symmetry coordinates. From these derivatives, the complete set of lines located in the range $1150 - 1460$ cm^{-1} is calculated. Therefore, this work could help in the quantitative diagnostics of combustion flames [5]. Our approach is consistent with the previous

analysis of the vibrational excitations of CO_2, where symmetry coordinates are first substituted by the corresponding bosonic creation and annihilation operators, and then a canonical transformation is applied in order to introduce local operators which are subsequently anharmonized. In this way, the advantages of a local-mode model are incorporated.

The outline of the present letter is as follows. In Section 2 we sketch the basic ingredients involved in the algebraic model to obtain the eigenstates in terms of basis of local states. Section 3 is devoted to the estimation of the derivatives of the polarizability tensor and to the comparison of theoretical and experimental results for CO_2 Raman spectrum. Finally, in Section 4, our conclusions are presented.

2. Algebraic approach

A possible approach to describe the vibrational excitations of carbon dioxide consists in expanding the kinetic and potential energy operators in terms of internal symmetry coordinates, labeled in shorthand as $\Sigma_{g/u}$ for the stretching modes and $+/-$ for the bending modes [1, 2]

$$\mathcal{Q}_{\Sigma_g} = \frac{1}{\sqrt{2}}\,(q_1 + q_2)\,, \qquad \mathcal{Q}_{\Sigma_u} = \frac{1}{\sqrt{2}}\,(q_1 - q_2) \quad , \tag{1a}$$

$$\mathcal{Q}_{+} = -\frac{1}{\sqrt{2}}\,(q_a + iq_b)\,, \quad \mathcal{Q}_{-} = \frac{1}{\sqrt{2}}\,(q_a - iq_b) \quad . \tag{1b}$$

For the stretching degrees of freedom $q_i = \Delta r_i = r_i - r_e$, with $i = 1, 2$. The quantity r_i is the i-th CO bond length, and $r_e = 1.1615$ Å is the equilibrium bond length. In the case of the doubly degenerate bending mode [9]

$$q_a = r_e\ \mathbf{e}_Y \cdot \frac{\mathbf{r_1} \times \mathbf{r_2}}{r_1 r_2} \quad , \quad q_b = -r_e\ \mathbf{e}_X \cdot \frac{\mathbf{r_1} \times \mathbf{r_2}}{r_1 r_2} \quad , \tag{2}$$

where $\mathbf{r_1}$ and $\mathbf{r_2}$ are vectors from the C-atom to each one of the O-atoms. The unit vectors $\mathbf{e}_X$ and $\mathbf{e}_Y$ lie on the direction of the X and Y-axis of the axis system, with its origin at the molecule's center of mass.

Thus the molecular Hamiltonian takes the form

$$\hat{H} = \hat{H}(\mathcal{P}_{\Sigma_g}, \mathcal{P}_{\Sigma_u}, \mathcal{P}_{\pm}, \mathcal{Q}_{\Sigma_g}, \mathcal{Q}_{\Sigma_u}, \mathcal{Q}_{\pm}) \quad , \tag{3}$$

whose explicit expression in terms of the symmetry coordinates $\mathcal{Q}$'s and their conjugate momenta $\mathcal{P}$'s is given by Eqs. (10)–(13) of Ref. [2]. An algebraic representation of this Hamiltonian is obtained through the introduction of bosonic creation and annihilation operators [1, 2]

$$a_\Gamma^\dagger = \alpha^\Gamma \mathcal{Q}_\Gamma - \frac{i}{2\hbar\alpha^\Gamma}\mathcal{P}_\Gamma \ , \quad a_\Gamma = \alpha^\Gamma \mathcal{Q}_\Gamma + \frac{i}{2\hbar\alpha^\Gamma}\mathcal{P}_\Gamma \quad ;\Gamma = \Sigma_g, \Sigma_u \quad , \tag{4a}$$

$$a_\pm^\dagger = \alpha^\pm \mathcal{Q}_\pm + \frac{i}{2\hbar\alpha^\pm}\mathcal{P}_\mp \ , \quad a_\pm = -\alpha^\pm \mathcal{Q}_\mp + \frac{i}{2\hbar\alpha^\pm}\mathcal{P}_\pm \quad . \tag{4b}$$

where α^Γ and $\alpha^\pm$ are given by Eqs. (16) and (18) in Ref.[1].

The algebraic representation of Eqs. (4) implies that the symmetry coordinates of Eq. (1) are truncated into rectilinear ones and therefore cannot be directly compared to the curvilinear coordinates in Ref.[6]. Hence, the obtained Hamiltonian can be diagonalized in a basis set built as the direct product of harmonic oscillator functions of the symmetry coordinates. An alternative approach is to carry out the diagonalization in a local basis, although this cannot be done in a straightforward way. The CO_2 molecule has a strong normal-mode behavior and an intense Fermi resonance. Due to its normal-mode character, its direct description from a local-mode scheme is not correct [1]. This issue can be overcome introducing the canonical transformation

$$a_{\Sigma_g}^\dagger = \frac{1}{\sqrt{2}}(a_1^\dagger + a_2^\dagger) \quad , \quad a_{\Sigma_u}^\dagger = \frac{1}{\sqrt{2}}(a_1^\dagger - a_2^\dagger) \quad , \tag{5}$$

where $a_i^\dagger(a_i)$ are also bosonic operators, associated with the i-th stretching local mode. It is appropriate to emphasize that the local operators $a_i^\dagger(a_i)$ do not exactly correspond to the physical local operators, but their action on an isomorphic local basis may be chosen to be the same (e.g. see App. B in Ref. [1]).

The diagonalization can be now carried out in a local basis defined in terms of the direct product of harmonic local oscillators. A convenient improvement is achieved with the introduction of the anharmonization procedure [1, 2, 10]

$$a_i^\dagger \to b_i^\dagger, \qquad a_i \to b_i \quad , \tag{6}$$

with $i = 1, 2$. The creation and annihilation operators $b_i^\dagger(b_i)$ are generators of a $U(2)$ dynamical algebra [11]. The operators $b_i^\dagger(b_i)$ can be interpreted as ladder operators for

a Morse potential eigenstates, $|\Psi^j_{v_i}\rangle$, with matrix elements [12]

$$b^\dagger|\Psi^j_v\rangle = \sqrt{(v+1)(1-(v+1)/\kappa)}\ |\Psi^j_{v+1}\rangle \quad , \tag{7a}$$

$$b\ |\Psi^j_v\rangle = \sqrt{v(1-v/\kappa)}\ |\Psi^j_{v-1}\rangle \quad , \tag{7b}$$

where v is the stretching quantum number, taking values $v = 0, 1, \ldots, j-1$, and $\kappa = 2j+1$ is related to the potential depth.

In the bending case, an equivalent anharmonization procedure is performed

$$a^\dagger_\pm \to b^\dagger_\pm, \qquad a_\pm \to b_\pm \quad , \tag{8}$$

but now the operators $b^\dagger_\pm(b_\pm)$ are generators of a $U(3)$ dynamical algebra [13], with matrix elements [1]

$$b^\dagger_\pm|[N];n^\ell\rangle = \sqrt{\left(\frac{n\pm\ell}{2}+1\right)\left(1-\frac{n}{N}\right)}\ |[N];(n+1)^{\ell\pm1}\rangle \quad , \tag{9a}$$

$$b_\pm|[N];n^\ell\rangle = \sqrt{\left(\frac{n\pm\ell}{2}\right)\left(1-\frac{n-1}{N}\right)}\ |[N];(n-1)^{\ell\mp1}\rangle \quad , \tag{9b}$$

where n and ℓ are the number of vibrational quanta and of the vibrational angular momentum, respectively. The harmonic 2D oscillator matrix elements are recovered in the large N limit of Eq. (9).

The anharmonization procedure replaces every creation $a^\dagger$ and annihilation a operator by the corresponding b operator (Eqs. 6 and 8) except the bending vibrational number of quanta and angular momentum operators, $\hat{n}$ and $\hat{\ell}$ defined as follows:

$$\begin{aligned} \hat{\ell} &= a^\dagger_+ a_+ - a^\dagger_- a_- = \hat{n}_+ - \hat{n}_- \quad , \\ \hat{n} &= a^\dagger_+ a_+ + a^\dagger_- a_- = \hat{n}_+ + \hat{n}_- \quad . \end{aligned} \tag{10}$$

Thus the algebraic Hamiltonian takes the general form [1, 2]

$$\hat{H} = \tilde{\omega}_s \sum_{k=1}^{2}\left(b^\dagger_k b_k + b_k b^\dagger_k\right) + \lambda_s \sum_{k\neq j=1}^{2} b^\dagger_k b_j + \alpha^s_1 \sum_{k=1}^{2}\left(b^\dagger_k b_k\right)^2$$

$$
\begin{aligned}
&+ \alpha_2^s \left(b_1^{\dagger 2} b_2^2 + b_2^{\dagger 2} b_1^2 + 4 b_1^\dagger b_2^\dagger b_1 b_2 \right) + \alpha_3^s \left[b_1^\dagger b_2^\dagger (b_1^2 + b_2^2) + H.c. \right] \\
&+ \tilde{\omega}_b \hat{n} + \alpha_1^b \hat{n}^2 + \alpha_2^b \hat{\ell}^2 + \alpha_1^{sb} \left\{ \left(b_1^\dagger + b_2^\dagger \right) b_+ b_- + H.c. \right\} \\
&+ \alpha_2^{sb} \left(b_1^\dagger b_1 + b_2^\dagger b_2 \right) \hat{n} + \alpha_3^{sb} \left(b_1^\dagger b_2 + b_2^\dagger b_1 \right) \hat{n} \quad . \qquad (11)
\end{aligned}
$$

Only those interactions that preserve the polyad number $P = 2(v_1 + v_2) + n$ enter into the model Hamiltonian. The Hamiltonian (11), after carrying out the anharmonization procedure given in Eqs. (6) and (8), is diagonalized in the basis $|\psi_{v_1}^j\rangle \otimes |\psi_{v_2}^j\rangle \otimes |N; n^\ell\rangle$. The spectroscopic parameters are optimized by an iterative non-linear least square method [14]. The potential depth parameter κ and the boson number N are initially estimated according to the system anharmonicity and were later manually adjusted to improve the results. The diagonalization of the Hamiltonian matrix, split into symmetry blocks, with the optimum set of parameters gives rise to a set of eigenvectors

$$
|P; \nu_1, \nu_2^\ell, \nu_3; \Gamma, \gamma\rangle = \sum_{v_1, v_2, n, \ell} C_{v_1, v_2, n, \ell}^{P; \nu_1, \nu_2, \nu_3; \Gamma, \gamma} \; |\psi_{v_1}^j\rangle |\psi_{v_2}^j\rangle |N; n^\ell\rangle \quad , \qquad (12)
$$

where Γ and γ label the irreducible representation and component, respectively, and the set $\{\nu_1, \nu_2^\ell, \nu_3\}$ is the traditional labeling for the vibrational states of a linear triatomic molecule in terms of its normal modes. In this scheme, the polyad number takes the form $P = 2(\nu_1 + \nu_3) + \nu_2$. It should be clear that the latter are approximate quantum numbers, obtained once the symmetrization procedure is carried out [15, 16]. The wavefunctions (12) obtained with this anharmonic algebraic procedure are close to those given in Table I of Ref. [6].

The Hamiltonian (11) was used in Refs. [1] to fit 101 vibrational levels with a rms deviation of 0.53 cm^{-1}. The value for the Fermi interaction coefficient was $\alpha_1^{sb} = 36.005$ cm^{-1}, with the corresponding estimated force constant $f_{q_1 q_a q_a} = -5.40$ aJÅ^{-3}. This value was far from the force constant $f_{q_1 q_a q_a} = -0.8841$ aJÅ^{-3} obtained by Chedin [17]. Here in a new fit [2] we have found another minimum, with similar values for all parameters but the one corresponding to the Fermi interaction, $\alpha_1^{sb} = -36.002$ cm^{-1}, which has a similar absolute value but opposite sign. This new fit provides a force constant $f_{q_1 q_a q_a} = -0.9551$ aJÅ^{-3}, which is now comparable to Chedin' s constant. Such a change of sign in the Fermi force constant has a large effect on the wavefunctions

which in turn shows up into the spectral transition intensities.

3. The calculated Raman spectrum

Line intensities in a Raman spectrum for a gas sample are given by the transition moments of the molecular polarizability tensor α. In the particular case of the CO_2 molecule, the non-vanishing components of α tensor have symmetries Σ_g^+ (trace) and $\Sigma_g^+ \oplus \Pi_g \oplus \Delta_g$ (anisotropy). The sharp, polarized, Q-branches in the vibrational Raman spectrum of CO_2 in the ~ 1300 cm^{-1} region are totally symmetric (Σ_g^+) transitions and their intensities are mainly due to the trace of the α tensor (mean-polarizability). For the trace scattering of a gas sample at thermal equilibrium, the differential cross section can be expressed in the SI system as follows [6]

$$\left(\frac{\partial\sigma}{\partial\Omega}\right)_{i\to f}^{\text{trace}} = \left(\frac{\pi}{\epsilon_0}\right)^2 \frac{(\nu_0+\nu_i-\nu_f)^4}{Z_{vib}(T)} g_{if}\,(M_{if})^2 \exp\left(-hc\nu_i/k_BT\right) \quad , \tag{13}$$

where ϵ_0 is the vacuum permitivity, ν_0 is the wave number of the exciting radiation, ν_i and ν_f are the wavenumbers of initial and final states, and g_{if} is the vibrational degeneracy of the transition. $Z_{vib}(T) = \sum_j g_j e^{-\nu_j/k_BT}$ is the vibrational partition function at the temperature T of the gas sample, where g_j is the degeneracy of the states with ν_j energy, and $M_{if} = \langle\nu_i|\bar{\alpha}|\nu_f\rangle$ is the transition moment of the mean molecular polarizability $\bar{\alpha}$ between vibrational states $|\nu_i\rangle$ and $|\nu_f\rangle$.

To compute the intensity (13) the molecular polarizability surface is needed. This surface is usually expressed as a Taylor series on the vibrational coordinates. The polarizability derivatives can be determined from *ab initio* calculations [18, 19] or, more frequently, empirical values can be obtained from a fit to experimental transition moments [6, 20].

In this work, the mean polarizability will be expanded in terms of our symmetry coordinates (1) up to cubic order as follows

$$\bar{\alpha} = \bar{\alpha}_0 + \left(\frac{\partial\bar{\alpha}}{\partial\mathcal{Q}_{\Sigma_g^+}}\right)_0 \mathcal{Q}_{\Sigma_g^+} + \frac{1}{2}\left(\frac{\partial^2\bar{\alpha}}{\partial\mathcal{Q}_{\Sigma_g^+}^2}\right)_0 \mathcal{Q}_{\Sigma_g^+}^2 + \frac{1}{2}\left(\frac{\partial^2\bar{\alpha}}{\partial\mathcal{Q}_{\Sigma_u^+}^2}\right)_0 \mathcal{Q}_{\Sigma_u^+}^2$$

$$+\frac{1}{2}\Big(\frac{\partial^2\bar{\alpha}}{\partial q_a^2}\Big)_0(q_a^2+q_b^2)+\frac{1}{2}\Big(\frac{\partial^3\bar{\alpha}}{\partial\mathcal{Q}_{\Sigma_g^+}\partial q_a^2}\Big)_0\mathcal{Q}_{\Sigma_g^+}(q_a^2+q_b^2)$$
$$+\frac{1}{2}\Big(\frac{\partial^3\bar{\alpha}}{\partial\mathcal{Q}_{\Sigma_g^+}\partial\mathcal{Q}_{\Sigma_u^+}^2}\Big)_0\mathcal{Q}_{\Sigma_g^+}\mathcal{Q}_{\Sigma_u^+}^2 \quad . \tag{14}$$

The last term in Eq. (14) turns out to be negligible and, consequently, it will be omitted [6].

The next task consists in computing the matrix elements of the mean molecular polarizability $\bar{\alpha}$ between the system wavefunctions (12). This is not straightforward since the eigenstates (12) are given in terms of local basis functions, while the expansion (14) involves symmetry coordinates. This difficulty disappears if we follow the same approach leading to Eq. (11). First we obtain an algebraic representation of $\bar{\alpha}$ introducing the bosonic operators (4). We then carry out an anharmonization through a canonical transformation. As an example, we apply this procedure to the second term in Eq. (14). The first step of the approach yields

$$\left(\frac{\partial\bar{\alpha}}{\partial\mathcal{Q}_{\Sigma_g^+}}\right)_0\mathcal{Q}_{\Sigma_g^+}=\left(\frac{\partial\bar{\alpha}}{\partial\mathcal{Q}_{\Sigma_g^+}}\right)_0\frac{1}{\sqrt{2}}\sqrt{\frac{\hbar}{\omega_{\Sigma_g^+}\mu_{\Sigma_g^+}}}(a_{\Sigma_g^+}^\dagger+a_{\Sigma_g^+}) \quad , \tag{15}$$

where ω is the harmonic frequency and μ the reduced mass of the vibration.

The symmetry coordinates can be expressed as power series expansions of the normal coordinates [9], whose linear terms are proportional to the corresponding normal coordinates. As previously stated after Eqs. (4), here that power series is cut off after first order and each symmetry coordinate is approximated to its normal coordinate. Consequently, the polarizability derivatives in Eq. (14) are proportional to their derivatives with respect to the normal coordinates. However, our approach improves the spectral description by introducing the canonical transformation in Eq. (5), followed by the anharmonization in Eqs. (6) and (8), to obtain

$$\left(\frac{\partial\bar{\alpha}}{\partial\mathcal{Q}_{\Sigma_g^+}}\right)_0\mathcal{Q}_{\Sigma_g^+}=\left(\frac{\partial\bar{\alpha}}{\partial\mathcal{Q}_{\Sigma_g^+}}\right)_0\frac{1}{2}\sqrt{\frac{\hbar}{\omega_{\Sigma_g^+}\mu_{\Sigma_g^+}}}(b_1^\dagger+b_1+b_2^\dagger+b_2). \tag{16}$$

The matrix elements of these operators in the local basis (12) are now well defined. The transition moments $M_{if}=|\langle\nu_i|\bar{\alpha}|\nu_f\rangle|$ can now be calculated using the expansion (14) and the wavefunctions (12). The comparison of the calculated M_{if}^{calc} with those

M_{if}^{exp} derived from the experimental transition intensities (13) [6, 21], allows us to obtain estimates of the molecular polarizability derivatives of Eq. (14). We thus define the root mean square deviation

$$rms = \sqrt{\sum_{\beta} [\log |M_{\beta}^{exp}| - \log |M_{\beta}^{calc}|]^2} \tag{17}$$

which is minimized by a suitable selection of the polarizability derivatives, using the values in Ref. [6] as initial guesses for the fitting procedure. The subindex β runs over the first six transitions displayed in Tab. 1. In this table the experimental and calculated wavenumbers of the Raman transitions, the available experimental matrix elements M_{if}^{exp} [6, 21], and the calculated values after the minimization of Eq. (17), as well as the states involved in the transitions following the notation (12), are given. In order to check the predictive power of our model, in the lower half of Tab. 1 we compare other four calculated transition moments with their experimental ones. It can be seen that all transition moments are well reproduced, even those not included in the fit. In Table 1, vibrational states are labelled according to their dominant component in the normal-mode basis set. However, due to the strong Fermi resonance, two states may carry the same labeling. For example, the vibrational states at 2548.4 and 2797.1 cm^{-1} are assigned to the same basis function $|4; 120; \Sigma_g^+\rangle$, but both states present a large contribution of $|4; 04^0 0; \Sigma_g^+\rangle$. The same situation occurs with the two states labelled as $|5; 130; \Pi_u\rangle$, which present a strong mixing with $|5; 05^1 0; \Pi_u\rangle$.

The derivatives of $\bar{\alpha}$ with respect to symmetry coordinates obtained in this work are displayed in the left panel of Tab. 2 and compared with *ab initio* and experimental values. In general, there is a good agreement between our results and the experimental and *ab initio* polarizability derivatives. The only significant discrepancies appear in the bending polarizability derivatives which stems from the different nature (rectilinear vs. curvilinear) of the employed coordinates.

It is also interesting to compare our results with the mean polarizability derivatives with respect to dimensionless normal coordinates obtained by *Tejeda et al.* in Ref. [6] (right panel of Tab. 2). For this purpose, the derivatives with respect to the symmetry coordinates of this work are transformed into dimensionless normal coordinates through

Eqs.(9) of Ref.[9], i.e. using the linear approximation in the power series expansion. The second derivative with respect to the bending coordinate, $\bar{\alpha}''_{+-}$, deserves some comments. Although its value has the same order of magnitude than the experimental value of *Tejeda et al.* it is a 31 % smaller. This is attributed to the different approaches used in this work and in Ref. [6]. In our case, the derivatives with respect to the rectilinear symmetry coordinates were fitted with eigenstates provided by the algebraic approach. In Ref.[6] the derivatives with respect to the normal coordinates were fitted using perturbation theory through the eigenfunctions of Chedin's work [17]. It is worth mentioning that if the latter procedure is applied to our calculated transition moments in Tab. 1, the value of $\bar{\alpha}''_{+-} = 2.28 \times 10^{-42}$ C m^2 V^{-1} is obtained, very close to the value 1.925×10^{-42} C m^2 V^{-1} of our fit. This is an indication of the consistency of the methodology employed in this work.

Considering the good results obtained for the vibrational energies (see Tab. 1 in Ref. [2]) and for the transition moments of the polarizability (see Tab. 1) we are confident to use the expansion (14) along with the model presented in Ref. [1, 2] to simulate the Raman spectrum of CO_2 at high temperature. In Fig. 1 we present the calculated spectrum of carbon dioxide at 1750 K in the wavenumber range $1150-1460$ cm^{-1}, along with the experimental one [5]. The procedure to obtain the synthetic spectrum consists in calculating the transition moments between the involved vibrational states with the same symmetry when the energy differences fall in the range of energies experimentally scanned. Then, scattering cross sections are calculated through Eq. (13), setting the vibrational degeneracy $g_{ij} = 1$ for the Σ states and $g_{ij} = 2$ for all the other symmetries. In order to simulate the spectrum in Fig. 1, experimental wavenumbers were used when available, and the transition lines are convoluted using a Gaussian profile up to the experimental bandwidth (1.2 cm^{-1}). To our knowledge, this is the first time that a simulated Raman spectrum of CO_2 at such a high temperature is reported. The good agreement between our simulated and the experimental spectra supports the quality of the wavefunctions obtained in this work even for highly excited vibrational levels.

4. Summary and conclusions

In this letter we have presented an approach to describe the Raman spectrum of the CO_2 molecule by means of a model based on unitary algebras, keeping the connection with configuration space. The most remarkable feature of this algebraic model is that a molecule with a strong normal-mode character can be described from a local-mode perspective. In particular, the CO_2 molecule, with an intense Fermi resonance besides a strong normal-mode behaviour, has been described obtaining a good energy fit and a correct estimation of the potential energy surface. The local-mode description is introduced via a canonical transformation which, after an anharmonization procedure, gives rise to the $U(2) \times U(3) \times U(2)$ model. The model basis set is built as the direct product of two 1D local Morse potential wavefunctions for the stretching and a 2D quasi-rigid bender wavefunction.

The present approach starts with the set of eigenvalues and eigenstates for CO_2 obtained with the aforementioned algebraic model. The polarizability function is first expanded in terms of symmetry coordinates, which later on is transformed to an algebraic representation by means of the creation and annihilation operators associated with the normal modes, by considering the linear approximation of the expansion of the symmetry coordinates in terms of the normal coordinates. After this step, a local algebraic representation is obtained through a canonical transformation that allows the anharmonization process to be applied. This makes possible to compute the Raman transition matrix elements using the algebraic eigenstates. An improvement of this approach is expected when higher order terms in the symmetry coordinates expansion were considered.

The CO_2 Raman spectrum has been simulated close to the experimental spectroscopic accuracy through a fit of the derivatives of the mean polarizability with respect to the symmetry coordinates. The polarizability derivatives obtained in this work agree with previous *ab initio* and experimental determinations. The eigenstates provided by the Hamiltonian parameter values in Ref. [2] along with the polarizability derivatives allow us to reproduce most of the available experimental Raman intensities. This is a

stringent test for the calculated wavefunctions opening up the possibility of simulations of high temperature Raman spectra of CO_2 for combustion flames diagnostics.

The present results are a nice example of a situation where a phenomenological model may give different outcomes having the same agreement with experimental energies, but implying a different molecular state behavior. The calculation of transition line intensities allows to elucidate which outcome provides the correct eigenstates. A similar situation has appeared in the calculation of Franck-Condon transition intensities [22].

The current approach could in principle be extended to deal with more complex molecular systems presenting either a local-mode or a normal-mode behavior, or even to open shell systems. Although algebraic methods are usually applied phenomenologically, our approach to describe vibrational excitations relies on expressing the Hamiltonian in the space of coordinates and momenta. This means that when vibronic or spin-orbit interactions are involved our approach may be applied as long as the Hamiltonian can be expressed as a convergent series in terms of the normal coordinates. In cases where the Born-Oppenheimer approximation is broken, our approach is not expected to provide a good description of the system. In such cases, *ab initio* calculations play a fundamental role [7, 8].

Finally, it should be reminded that our approach, like all methods based on effective Hamiltonians, is partially empirical in the sense that experimental energies and transition intensities are needed to fit a number of parameters. Thus, the accuracy of the method relies on the quality of the input data, and in principle we are unable to predict vibrational energy or intensity patterns for yet unknown systems. However, since our algebraic approach is connected with the space of coordinates and momenta, some predictions are possible as long as force constants and dipole moment or polarizability derivatives are available. The present work can be representative of such a capability, since by using only six experimental transition moments as input data for the Raman intensities, the full spectrum at high temperature, involving a lot of excited states, is satisfactorily simulated.

Acknowledgements. This work has been partially supported by CONACyT, México, by Junta de Andalucía (Spain) through contract no. P07-FQM-03014 and P07-FQM-02962. We also acknowledge funding support from the Spanish MEC through grant FIS2010-22064-C02 and FIS2011-28738-C02-02. Thanks are due to J. Ortigoso for helpful comments on the manuscript.

References

[1] M. Sánchez-Castellanos, R. Lemus, M. Carvajal and F. Pérez-Bernal, *J. Mol. Spectrosc.* **253** (2009) 1-15.

[2] M. Sánchez-Castellanos, R. Lemus, M. Carvajal and F. Pérez-Bernal, *Int. J. Quant. Chem.* **112** (2012) 3498-3507.

[3] A. Frank, R. Lemus, R. Bijker, F. Pérez-Bernal and J.M. Arias, *Ann. of Phys.***252**(1996) 211-238.

[4] H. Ishikawa *et al.*, *Chem. Phys. Lett.* **365** (2002) 57-68.

[5] J.M. Fernández, A. Punge, G. Tejeda and S. Montero, *J. Raman Spectrosc.* **37** (2006) 175-182.

[6] G. Tejeda, B. Maté and S. Montero, *J. Chem. Phys.* **103** (1995) 568-576.

[7] M.Peric, S.Peyerimhoff, *Adv. Chem.Phys.* Vol. 124 (2002) 583-658.

[8] M.Perić, S. Jerosimić, R. Ranković, M. Krmar, J. Radić-Perić, *Chem.Phys.* Vol. 330 (2006) 60-72: Ibid. Vol. 330 (2006) 73-81.

[9] A.R. Hoy, I.M. Mills and G. Strey, *Mol. Phys.* **24** (1972) 1265-1290.

[10] O. Castaños and R. Lemus,*Mol. Phys.***108** (2010) 597-610.

[11] F. Iachello and R.D. Levine, *Algebraic Theory of Molecules*; Oxford University Press, Oxford, 1995.

[12] R. Lemus, *J. Mol. Spectrosc.* **225** (2004) 73-92.

[13] F. Iachello and S. Oss, *J. Chem. Phys.* **104** (1996) 6956-6963.

[14] P.J. Brussaard and P. W. M. Glaudemans, *Shell-model applications in Nuclear Spectroscopy*, North-Holland (1977).

[15] R. Lemus , *Mol. Phys.*, **101** (2003) 2511-2528.

[16] O. Álvarez-Bajo, R. Lemus, M. Carvajal and F. Pérez-Bernal, *Mol. Phys.*, **109** (2011) 797-812.

[17] A. Chedin and J.L. Teffo, *J. Mol. Spectrosc.* **107** (1984) 333-342.

[18] G. Maroulis, *Chem. Phys.* **291** (2003) 81-95.

[19] A. Haskopoulos and G. Maroulis, *Chem. Phys. Lett.* **417** (2006) 235-240.

[20] R. Akhmedzhanov, A.K. Atakhodzhaev, and M.O. Bulanin, *J. Mol. Struct. THEOCHEM* **89** (1982) 285-290.

[21] M. Chrysos, I.A. Verzhbitskiy, F. Rachet and A.P. Kouzov, *J. Chem. Phys.* **134** (2011) 104310 (6pp).

[22] T. Müller, P.H. Vaccaro, F. Pérez-Bernal, and F. Iachello, *J. Chem. Phys.* **111** (1999) 5038-5055.

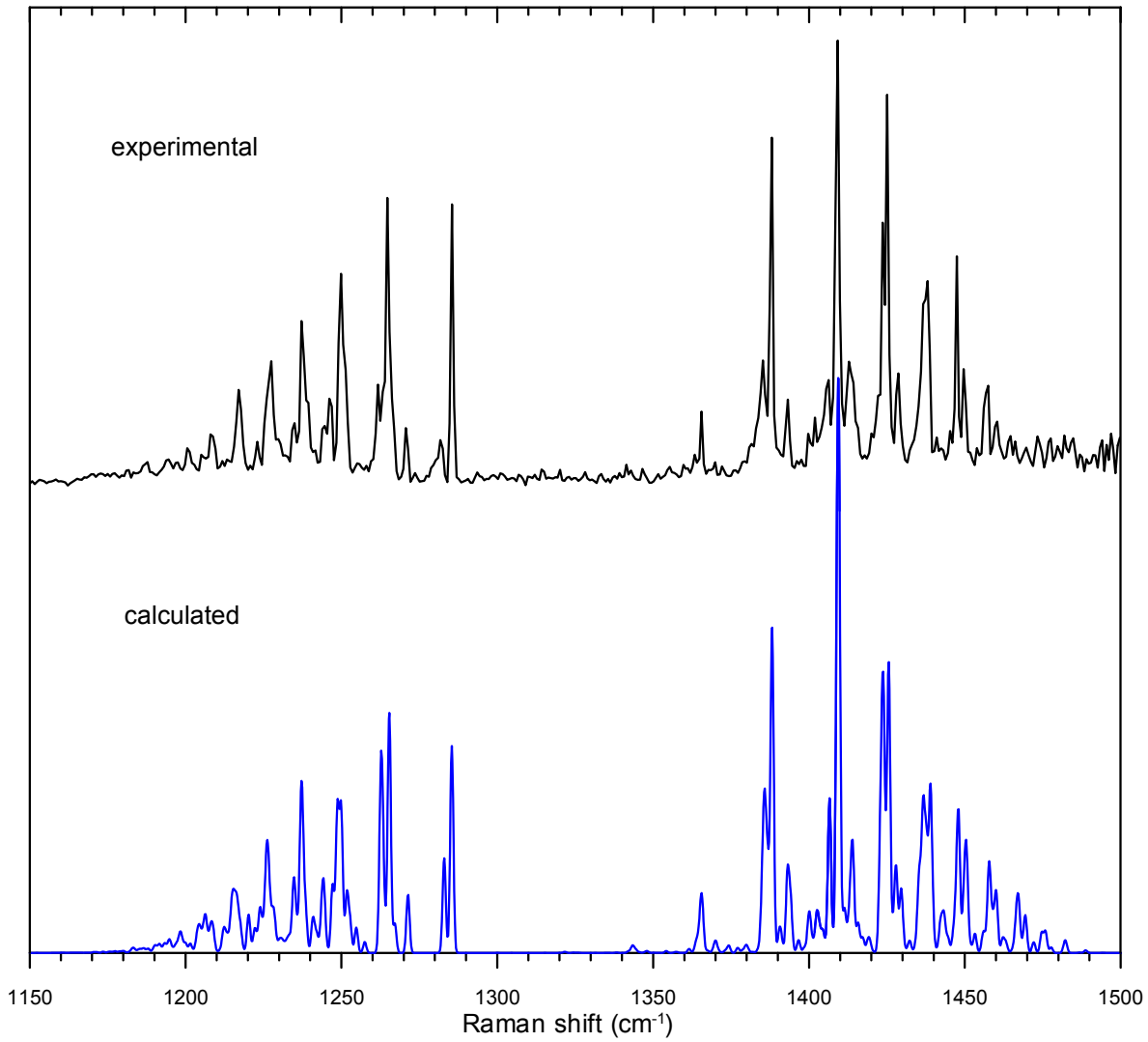

Figure 1: Experimental [5] and calculated Raman spectrum of CO_2 at 1750 K.

Table 1. Experimental and fitted transition moments $|M_{if}| = |\langle\nu_i|\bar{\alpha}|\nu_f\rangle|$ of the mean polarizability of CO_2. The first six transitions were involved in the fit while the last five are predictions. The labeling was chosen to be the normal mode scheme (ν_1, ν_2, ν_3).

ν $(\mathrm{cm}^{-1})^a$	ν $(\mathrm{cm}^{-1})^b$	$\|\nu_i\rangle^c \longrightarrow \|\nu_f\rangle$ transition	$\|M_{if}\| = \|\langle\nu_i\|\bar{\alpha}\|\nu_f\rangle\|^d$	$\|M_{if}\| = \|\langle\nu_i\|\bar{\alpha}\|\nu_f\rangle\|^e$
1285.4	1286.29	$\|0;000;\Sigma_g^+\rangle \longrightarrow \|2;100;\Sigma_g^+\rangle$	5.58	5.58
1388.2	1387.54	$\|0;000;\Sigma_g^+\rangle \longrightarrow \|2;020;\Sigma_g^+\rangle$	6.79	6.79
2548.4	2549.53	$\|0;000;\Sigma_g^+\rangle \longrightarrow \|4;120;\Sigma_g^+\rangle$	0.088	0.089
2671.1	2671.11	$\|0;000;\Sigma_g^+\rangle \longrightarrow \|4;200;\Sigma_g^+\rangle$	0.114	0.110
2797.1	2795.98	$\|0;000;\Sigma_g^+\rangle \longrightarrow \|4;120;\Sigma_g^+\rangle$	0.026	0.026
4673.3	4673.17	$\|0;000;\Sigma_g^+\rangle \longrightarrow \|4;002;\Sigma_g^+\rangle$	0.050^f	0.050
1265.1	1266.04	$\|1;010;\Pi_u\rangle \longrightarrow \|3;110;\Pi_u\rangle$	5.4	5.41
1409.5	1408.54	$\|1;010;\Pi_u\rangle \longrightarrow \|3;030;\Pi_u\rangle$	7.2	6.95
2514.1	2515.01	$\|1;010;\Pi_u\rangle \longrightarrow \|5;130;\Pi_u\rangle$	0.095	0.107
2671.9	2671.93	$\|1;010;\Pi_u\rangle \longrightarrow \|5;210;\Pi_u\rangle$	...	0.102
2833.3	2831.93	$\|1;010;\Pi_u\rangle \longrightarrow \|5;130;\Pi_u\rangle$	≤ 0.03	0.019

[a] Experimental transition wavenumber [6].

[b] Theoretical wavenumber calculated from the fitted vibrational term values of Ref. [2].

[c] The vibrational states are labeled by the ket $|P;\nu_1,\nu_2,\nu_3;\Gamma\rangle$ where P is the polyad number, (ν_1,ν_2,ν_3) are the quantum numbers of the dominant contribution in the normal-mode representation (see text) and Γ is the symmetry of the vibrational wavefunction.

[d] Experimental values from Ref. [6] in $10^{-42}\mathrm{CV}^{-1}\mathrm{m}^2$ otherwise is indicated.

[e] Fitted and predicted values of the transition moment in $10^{-42}\mathrm{CV}^{-1}\mathrm{m}^2$ obtained from this work.

[f] Value derived from *Chrysos et al.* [21].

Table 2. Derivatives of the mean polarizability of CO_2 with respect to the symmetry coordinates (left panel) and dimensionless normal coordinates (right panel).

Symmetry coordinates				Dimensionless normal coordinates		
Derivative (units) [a]	This work [b]	Ab initio [c]	Exp. [d]	Derivative [e] $(10^{-42}CV^{-1}m^2)$	This work [f]	Exp. [d]
$(\partial\bar{\alpha}/\partial\mathcal{Q}_{\Sigma_g})_0(10^{-30}\,CV^{-1}m)$	3.15	3.04	3.15	$\bar{\alpha}'_1$	12.44	12.43
$(\partial^2\bar{\alpha}/\partial\mathcal{Q}^2_{\Sigma_g})_0(10^{-20}\,CV^{-1})$	2.549	2.23	2.9	$\bar{\alpha}''_{11}$	0.398	0.45
$(\partial^2\bar{\alpha}/\partial\mathcal{Q}^2_{\Sigma_u})_0(10^{-20}\,CV^{-1})$	0.447	0.81	0.5 [g]	$\bar{\alpha}''_{33}$	0.144	0.15 [g]
$(\partial^2\bar{\alpha}/\partial q_a^2)_0(10^{-20}\,CV^{-1})$	0.8395		0.36	$\bar{\alpha}''_{+-}$	1.925	2.81
$(\partial^3\bar{\alpha}/\partial\mathcal{Q}_{\Sigma_g}\partial q_a^2)_0(10^{-10}\,CV^{-1}m^{-1})$	−1.21		−1.7	$\bar{\alpha}'''_{1+-}$	−0.110	−0.06

[a] Polarizability function derivatives as defined in Eq. (14).

[b] Values obtained in this work by a fitting of experimental polarizability transition moments (see Table 1).

[c] Refs. [18, 19].

[d] Experimental values [6].

[e] Polarizability function derivatives in terms of dimensionless normal coordinates as defined in Ref. [6].

[f] Polarizability derivative values given in second column after transforming them from symmetry coordinates to dimensionless normal coordinates.

[g] Best choice of the two available experimental values of *Tejeda et al.* [6] according to the *ab initio* CCSD(T) value provided in Ref. [19].